

# The Impact of Star Formation on Cool Core Galaxy Clusters

Patrick M. Motl,<sup>1</sup> Jack O. Burns,<sup>1</sup> Michael L. Norman,<sup>2</sup> and Greg L. Bryan<sup>3</sup>

<sup>1</sup> *University of Colorado, Center for Astrophysics and Space Astronomy, Boulder, CO 80309*

<sup>2</sup> *University of California San Diego, Center for Astrophysics and Space Sciences, 9500 Gilman Drive, La Jolla, CA 92093*

<sup>3</sup> *University of Oxford, Astrophysics, Keble Road, Oxford OX1 3RH*

We present results from recent simulations of the formation and evolution of clusters of galaxies in a  $\Lambda$ CDM cosmology. These simulations contain our most physically complete input physics to date including radiative cooling, star formation that transforms rapidly cooling material into aggregate star particles and we also model the thermal feedback from resulting supernovae in the star particles. We use an adaptive mesh refinement (AMR) Eulerian hydrodynamics scheme to obtain very high spatial resolution ( $\approx 2$  kpc) in a computational volume 256 Mpc on a side with mass resolution for dark matter and star particles of  $\approx 10^8 M_\odot$ . We examine in detail the appearance and evolution of the core region of our simulated clusters.

## 1. Description

We explore the role that star formation plays in shaping the appearance of gas in clusters of galaxies. If only radiative cooling is allowed to operate, nearly all halos in our simulations develop cores of cool, dense material at their center. Star formation provides a natural sink for this cool material and additionally, the feedback of energy from supernovae may impact the energy budget of some clusters and groups. In this poster, we describe our simulation efforts with star formation and demonstrate its impact by examining (1) the thermodynamic phase of material in representative simulations, (2) the run of entropy in simulated clusters and (3) the temperature profiles from samples of simulated clusters. We also present preliminary results from simulations where star formation is halted at a specific redshift. These simulations with truncated star formation yield promising results for the formation of realistic cool cores in clusters of galaxies. Also, there is a sequence of movies available that illustrate the evolution of one massive cluster at high resolution.

## 2. Simulations

We have constructed samples of simulated galaxy clusters using a sophisticated, Eulerian adaptive mesh refinement cosmology code that incorporate successively more sophisticated input physics. The simulations evolve dark matter particles and utilize the piecewise parabolic method to evolve the baryonic component. Each simulation sample contains the same clusters evolved with a specific set of physical assumptions at modest resolution (15.6 kpc). In our baseline adiabatic sample our simulations trace the gravitational heating as clusters assemble. At the next level of complexity, we include radiative cooling by the cluster gas. We use a tabulated cooling curve assuming a metal abundance of 0.3 solar. We have also generated cluster samples using a star formation algorithm similar to the scheme developed by Cen & Os-

triker (1992) that transforms rapidly cooling, collapsing gas into collisionless “star” particles. For the star formation samples, we consider both the case of star formation only and the case where the stars deposit thermal energy back into the neighboring gas.

Our star formation algorithm sweeps through the finest resolution grids every timestep and searches for cells with the following properties:

- Resides in a region of overdensity exceeding a threshold,  $\delta$
- Convergence of flow in the cell ( $\nabla \cdot \mathbf{v} < 0$ )
- The local cooling time is shorter than the local free fall time
- The mass of baryons in the cell exceeds the Jean’s mass.

If a cell that matches these conditions has enough material to exceed a minimum star particle mass (which is introduced to limit the number of star particles that must be evolved) then a new star is created with a mass  $m_\star = \eta m_{\text{baryon}} \Delta t / t_{\text{dynamical}}$ , where  $\Delta t$  is the simulation timestep and  $\eta$  is an efficiency parameter. If the minimum mass threshold is not met in this timestep, the code will track the frustrated attempt to form a star and the threshold can be exceeded incrementally. Once formed, the star begins to both heat the surrounding fluid to model the feedback from prompt supernovae and the star pollutes the fluid with a passive metallicity tracer field. The total energy deposited is scaled to the rest-mass energy of the star particle with an efficiency parameter,  $\epsilon$ .

Given the complexity of the star formation algorithm, we have run numerous simulations to explore the parameter space. Variations in the overdensity threshold,  $10 < \delta < 1 \times 10^4$ ; feedback strength,  $0 < \epsilon < 1 \times 10^{-4}$ ; star formation efficiency,  $0.01 < \eta < 1$ ; and minimum mass of the star particles (ranging from  $10^6 M_\odot$  to

$10^9 M_\odot$ ) do not significantly impact the properties of the baryons in clusters of galaxies. Roughly, the strength of feedback controls the amount of mass that is converted into stars and to a lesser degree, the overdensity threshold dictates when star formation begins in the simulation. Similarly, the efficiency of star formation will control the amount of mass converted into stars but to a lesser degree than the feedback strength. **On the scale of clusters however, the primary role of star formation is to allow rapidly cooling gas to leave the fluid.**

All simulations presented here were computed assuming a  $\Lambda$ CDM cosmological model with the following parameters:  $\Omega_b = 0.026$ ,  $\Omega_m = 0.3$ ,  $\Omega_\Lambda = 0.7$ ,  $h = 0.7$ , and  $\sigma_8 = 0.928$ . Each physics sample contains approximately 75 clusters in the mass range from  $4 \times 10^{14} M_\odot$  to  $2 \times 10^{15} M_\odot$  at the present epoch.

### 3. Baryon Distribution

Radiative cooling allows the baryonic fluid to lose energy, causing the material to lose pressure support and condense. With the addition of star formation, these cool condensations can be removed from the fluid. However, the gross thermodynamic state of the baryons is dictated by the structure formation process and only relatively small regions in the simulation have cooling times that are short on a cosmological timescale. Furthermore, it is only in these regions where star formation can act. As can be seen in Figure 1, the overall thermodynamic state of baryons in the simulations does not depend strongly on the input physics beyond the hierarchical collapse and shock heating present in the adiabatic limit. In highly overdense regions, such as the cores of clusters of galaxies, additional physics such as star formation play a significant role.

### 4. The Entropy Floor

The process of galaxy formation in the distant past is believed to have left a signature on the present day appearance of clusters and groups in the form of a universal entropy floor (Ponman et al. 1999). Gas at a lower entropy than this universal floor value should not appear in clusters as it would have been either heated to higher entropies by non-gravitational processes or either cooled to invisibility or collapsed into stars due to its short cooling time. In Figure 2 we show profiles of the fluid's entropy - normalized by the average cluster temperature - for 50 clusters evolved with star formation and a realistic amount of thermal feedback. The profiles have been color coded by the average cluster temperature as indicated in the figure caption. Most clusters have normalized core entropies at  $\approx 100 \text{ cm}^2$  and therefore, these systems approximately obey self-similar scaling ( $s \propto T$ ) in their cores. We do note that the variation of core entropy increases significantly for the cooler systems. A plot of entropy profiles for the sample without supernova feedback, meaning that the gas can collapse to form stars but these stars do not heat the remaining fluid, is very similar to that shown in Figure 2. This indicates that supernova feedback does not play a significant role in heating the cluster material, rather it is the case that fluid with entropy lower than the floor value is simply removed from

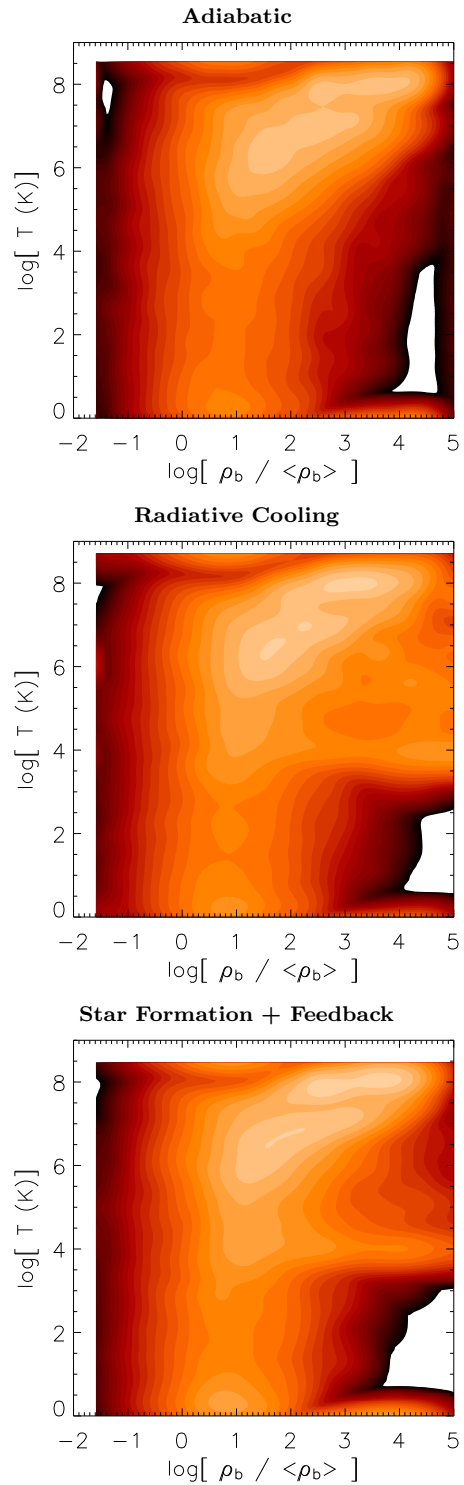


FIG. 1.— The thermodynamic phase of all gas cells in the refined region for three different sets of input physics at the present epoch. The contours are in the fraction of total mass in the volume at the indicated temperature and density. Note that the inclusion of star formation and feedback does not significantly alter the distribution of baryons.

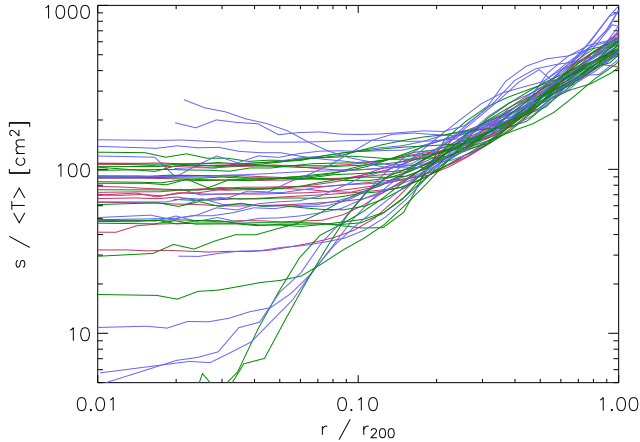


FIG. 2.— The entropy ( $s \equiv T/n_e^{2/3}$ ) scaled by the mean cluster temperature as a function of normalized radius for 50 clusters in the continuous star formation + feedback sample. The profiles are color-coded by the average temperature of the cluster with red denoting clusters with  $5 \text{ keV} < T_{\text{avg}} < 10 \text{ keV}$ , green for clusters with  $3.6 \text{ keV} < T_{\text{avg}} < 5 \text{ keV}$  and finally blue for clusters with  $2.4 \text{ keV} < T_{\text{avg}} < 3.6 \text{ keV}$ . The average cluster temperature is computed from the emission-weighted temperature within 0.3 virial radii for an overdensity of 200.

the system. A puzzle remains however as other forms of non-gravitational heating, such as feedback from AGN, would likely raise the core entropy beyond that observed. Yet, some physical mechanism must be acting to break self-similarity if an entropy scaling relation of the form  $s(0.1r_{\text{virial}}) \propto T^{0.65}$  as measured by Ponman et al. (2003) is correct.

### 5. Are There Cool Cores with Continuous Star Formation?

A crucial test of our simulations is whether they produce clusters with temperature structure similar to that in systems observed with *Chandra* and *XMM*. As a simple first step toward making this comparison, we examine the temperature profiles from our sample clusters. In Figure 3, we show the average profiles from 50 clusters evolved with adiabatic physics, radiative cooling, star formation and finally star formation with feedback. For both star formation samples, no cluster exhibits a cool core at the present epoch whereas a majority of observed clusters have cool cores. Instead, the individual cluster temperature profiles are flat or slightly rising toward the cluster center of mass. We have confirmed this result with simulations of individual clusters at higher resolution (up to 1 kpc) and with different input parameters for the star formation algorithm.

### 6. Truncated Star Formation

We have recently studied a simple extension to our standard star formation prescription that is meant to model the observed decay in global star formation rate at a redshift between 1 and 2. As a first approximation to enforcing this constraint on our simulations, we have simply turned off star formation at a given redshift and

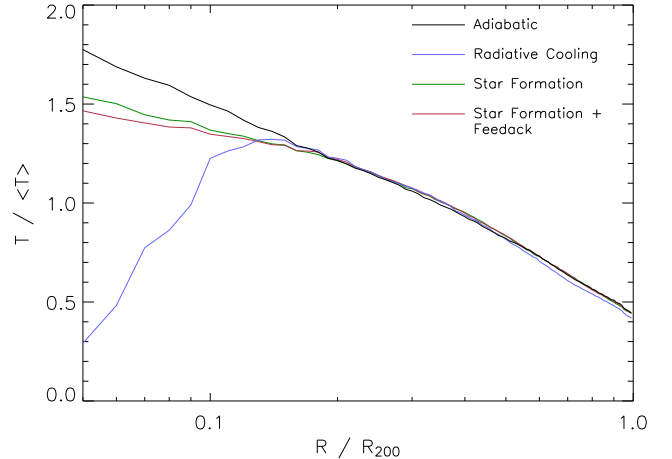


FIG. 3.— The average temperature profiles derived from the projected, emission-weighted temperature field for our four physics samples plotted against the normalized radius. The average temperature has been calculated within half a virial radius of the cluster center of mass.

allowed the simulation to complete with losses due to radiative cooling and, for consistency, with feedback from the star particles that have already formed. As can be seen in Figure 4, the epoch where star formation is truncated ( $z_{\text{truncation}}$ ) strongly influences the evolution of the cluster if it occurs in a narrow range between redshifts of 1.5 and 2. While these results are both preliminary and are calculated in a rather crude approximation, it is important to note that this approach represents the only means we have found to date for creating a realistic cool-core cluster with star formation, meaning a cluster with a core of material at about 1–2 keV.

### 7. Movie Description

We have prepared a series of animations for one particular cluster evolved with star formation and supernova feedback. The animations are available in mpeg format at the following URL: <http://casa.colorado.edu/~motl/research>. The simulation was run with 10 levels of refinement yielding a peak spatial resolution of slightly less than 2 kpc and with the following parameters for the star formation algorithm (see the discussion of the simulation technique above for a description of these parameters):  $\delta = 100$ ,  $\eta = 0.1$ ,  $\epsilon = 4.1 \times 10^{-6}$ , and a minimum star particle mass of  $1 \times 10^7 M_{\odot}$ . In addition, we assume that a given star particle will lose one quarter of its initial mass during supernova feedback and that the ejecta is polluted with metals at solar abundance (2% by mass). The simulation evolves a box approximately 40 Mpc on a side with adaptive mesh refinement within a volume 256 Mpc on a side. In the movies, we show a much smaller region 8 Mpc on a side at the present epoch that is centered about the final cluster center of mass. Scalar quantities of interest for the cluster at a redshift of zero are listed in the following table. The virial overdensity is taken to be 200. Masses are integrated out to the virial radius, as is the X-ray luminosity which is calculated for the 1 to

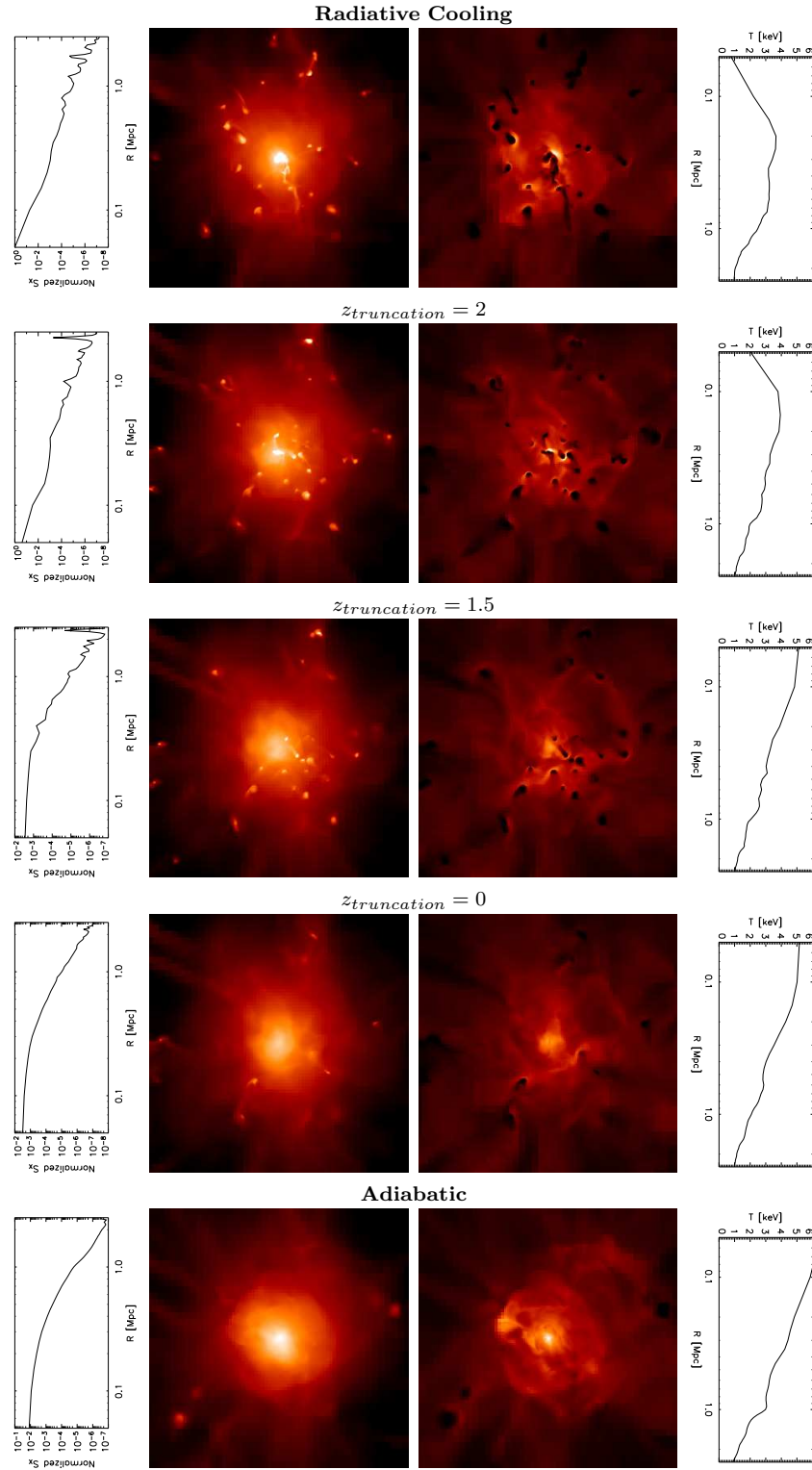


FIG. 4.— Images of X-ray surface brightness and projected, emission-weighted temperature maps at the present epoch for the same cluster run in the adiabatic and radiative cooling limits as well as with star formation + feedback for a range of truncation values. Each image is 5 Mpc on a side. Profiles of the normalized X-ray surface brightness and projected temperature are shown in the far left and right columns. If star formation is truncated at redshifts higher than 2, the cluster forms a cool core. If, however, star formation continues past a redshift of 1.5 no gas remains with a sufficiently short cooling time to form a cool core at the present epoch.

TABLE 1.

Param.	Value	Param.	Value
$R_{\text{virial}}$	$2.6 \text{ Mpc}$	$L_X$	$2.9 \times 10^{44} \text{ erg s}^{-1}$
$M_{\text{virial}}$	$2.1 \times 10^{15} M_{\odot}$	$T_{\text{avg}}$	$6.1 \text{ keV}$
$M_{\text{dm}}$	$2.0 \times 10^{15} M_{\odot}$	$T_{\text{core}}$	$14 \text{ keV}$
$M_{\text{gas}}$	$9.8 \times 10^{13} M_{\odot}$	$t_{\text{cool}}$	$8.7 \times 10^{10} \text{ years}$
$M_{\star}$	$2.1 \times 10^{13} M_{\odot}$	$\sigma$	$2,100 \text{ km s}^{-1}$

10 keV band.  $T_{\text{avg}}$  is the average, emission-weighted temperature out to the virial radius while  $T_{\text{core}}$  is measured over the central 50 kpc only. The central cooling time is given as  $t_{\text{cool}}$  and  $\sigma$  is the three-dimensional average velocity dispersion.

## 8. Conclusion

For our chosen star formation prescription with **continuous star formation**, no cluster has a cool core at the present epoch despite variation of the star formation parameters and increasing the simulation resolution by a factor of 16. However, in recent calculations, **the truncation of star formation** at an epoch between redshifts of 1.5 and 2 produces a realistic cool-core cluster.

This research was partially supported by grant TM3-4008A from NASA. The simulations presented in this poster were conducted on the Origin2000 system at the National Center for Supercomputing Applications at the University of Illinois, Urbana-Champaign through computer allocation grant AST010014N.

## References

- Cen, R. & Ostriker, J. P. 1992, ApJ, 399, L11  
 Ponman, T. J., Cannon, D. B. & Navarro, J. F. 1999, Nature, 397, 135  
 Ponman, T. J., Sanderson, A. J. R. & Finoguenov, A. 2003, MNRAS, 343, 331